

# Au<sub>20</sub> Nanocluster Protected by Hemilabile Phosphines

Xian-Kai Wan, Zhi-Wei Lin, and Quan-Ming Wang\*

State Key Laboratory of Physical Chemistry of Solid Surfaces, Department of Chemistry, College of Chemistry and Chemical Engineering, Xiamen University, Xiamen, Fujian 361005, P. R. China

**S** Supporting Information

**ABSTRACT:** A novel phosphine-protected Au<sub>20</sub> nanocluster was isolated through the reduction of Au(PPhpy<sub>2</sub>)Cl by NaBH<sub>4</sub> (PPhpy<sub>2</sub> = bis(2-pyridyl)-phenylphosphine). Its composition was determined to be [Au<sub>20</sub>(PPhpy<sub>2</sub>)<sub>10</sub>Cl<sub>4</sub>]Cl<sub>2</sub>, and single crystal X-ray structural analysis revealed that the Au<sub>20</sub> core can be viewed as being generated from the fusion of two Au<sub>11</sub> clusters via sharing two vertices. Optical absorption spectroscopy indicated this Au<sub>20</sub> has a large HOMO–LUMO gap ( $E_g \approx 2.24$  eV). This is the first example of a ligand-protected gold nanocluster with a core generated from incomplete icosahedral Au<sub>11</sub> building units.

Gold-nanoclusters receive an intense interest due to their relevance to a variety of properties including luminescence, catalysis, and biological applications.<sup>1</sup> Ligand-protected gold nanoclusters having well-defined compositions and structures are of great significance in terms of the correlation of structures and properties. So far, a large number of ligand-protected gold clusters have been prepared, and mass spectrometry has been the main technique to identify their compositions.<sup>2</sup> Unambiguous determination of the structures of the clusters is a challenge due to the difficulties in obtaining X-ray quality single crystals. In this regard, significant advances have been made with thiolate-protected gold nanoclusters. The crystal structures of Au<sub>102</sub>,<sup>3</sup> Au<sub>25</sub>,<sup>4</sup> and Au<sub>38</sub><sup>5</sup> have been determined. Regarding phosphine-protected gold nanoclusters, the structures of small ones such as Au<sub>4–10</sub>, Au<sub>11</sub> and Au<sub>13</sub> are known,<sup>6</sup> and their formation mechanism and electronic structures have attracted recent attention.<sup>7,8</sup> However, there is only one structurally characterized phosphine-protected gold nanocluster beyond Au<sub>13</sub>, [Au<sub>39</sub>(PPh<sub>3</sub>)<sub>14</sub>Cl<sub>6</sub>]Cl<sub>2</sub>.<sup>9</sup>

Icosahedral Au<sub>13</sub> motif is an important basic unit for most known structures with nuclearity higher than 13. Au<sub>25</sub> was found having a structure with a Au<sub>13</sub> core with RS-Au-SR-Au-SR staples attached.<sup>4,10</sup> Homonuclear structures such as a vertex-sharing biicosahedra in [Au<sub>25</sub>(PPh<sub>3</sub>)<sub>10</sub>(SC<sub>2</sub>H<sub>5</sub>)<sub>5</sub>Cl<sub>2</sub>]<sup>2+</sup>,<sup>11</sup> a face fusing biicosahedra Au<sub>23</sub> in Au<sub>38</sub>(SR)<sub>24</sub> have been reported.<sup>5</sup> Cyclic triicosahedra<sup>12a</sup> and interpenetrated biicosahedra<sup>12b</sup> have been founded in Au–Ag mixed metal clusters. Herein, we report a structurally determined Au<sub>20</sub> cluster with a unique core structure, which can be viewed as the fusion of two incomplete icosahedral Au<sub>11</sub> units.

Both phosphines and thiolates have been used in the preparation of ligand-protected gold nanoclusters. Au–P bonds are weaker than Au–S bonds. Normally, a phosphine is neutral but a thiolate possesses a negative charge; phosphines are

terminal ligands, while thiolates can bridge gold centers. In an attempt to increase the stability of phosphine-protected gold nanoclusters, our synthetic strategy is the use of pyridyl phosphines. A pyridyl phosphine contains P and N donors, which makes it available for bridging two metal centers as well as protecting gold atoms.

Typically, to 3.5 mL of ethanol suspension containing 0.20 mmol Au(PPhpy<sub>2</sub>)Cl, a freshly prepared solution of NaBH<sub>4</sub> (0.05 mmol in 1 mL of ethanol) was added dropwise under vigorous stirring. The color was immediately changed from white to orange and to black. The reaction continued for 24 h at room temperature in air under the exclusion of light. A small amount of brown solid appeared at the flask bottom. Twenty milliliters of *n*-hexane was added to give a brown precipitate, which was collected by filtration. This crude solid was dissolved in a mixture of solvents containing 3 mL of CH<sub>2</sub>Cl<sub>2</sub> and 0.2 mL of methanol, and the resulting solution was subject to diffusion of ether to afford black crystals after ca. 10 days (7.2 mg yield 10.1% based on Au). The identity was determined to be [Au<sub>20</sub>(PPhpy<sub>2</sub>)<sub>10</sub>Cl<sub>4</sub>]Cl<sub>2</sub> (**1**). <sup>31</sup>P NMR shows one singlet at 52.2 ppm, which indicates the phosphines have fast dynamic behavior in solution. TGA indicated that the loss of the cocrystallized solvent molecules happened below 130 °C.

Single crystal structural analysis revealed that **1** crystallizes in triclinic with  $P\bar{1}$  space group.<sup>13</sup> It comprises a dicationic cluster [Au<sub>20</sub>(PPhpy<sub>2</sub>)<sub>10</sub>Cl<sub>4</sub>]<sup>2+</sup> and two chloride counteranions. The structure of the centrosymmetric cation is shown in Figure 1, which consists of a Au<sub>20</sub> core, 10 phosphines and four chloride ligands. The Au⋯Au distances from the interstitial atom to the surface ones are in the range of 2.6438(9)–2.815(1) Å except for a longer one being 2.992(1) Å, and the separation between two interstitial gold atoms is 3.141(1) Å. The waist of the core is clutched by four PN bridges, and the P and N donors of the phosphines are bound to two Au atoms (Figure 2a). Four chlorides are additionally coordinated to the cluster core with Au–Cl bond lengths being 2.365(5) and 2.375(6) Å.

The Au<sub>20</sub> skeleton could be viewed as the fusion of two Au<sub>11</sub> incomplete icosahedra. As illustrated in Figure 2b, two Au<sub>11</sub> clusters join together via the sharing of the green vertices to generate the Au<sub>20</sub> core structure, which results in the formation of five additional gold–gold bonds including four on edge and one connecting two interstitial gold atoms.

The sample was further characterized by a high-resolution Fourier transform ICR spectrometer with an electrospray ionization source in positive mode (Figure 3a). Although [Au<sub>20</sub>(PPhpy<sub>2</sub>)<sub>10</sub>Cl<sub>4</sub>]<sup>2+</sup> was not found, intense peaks at  $m/z =$

Received: July 24, 2012

Published: August 29, 2012

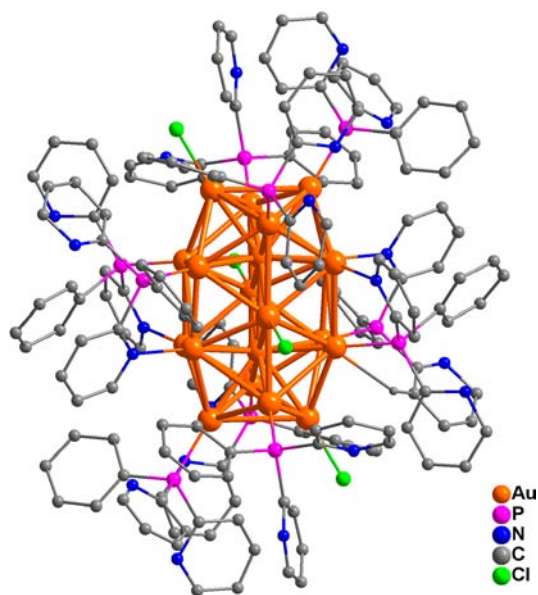


**Figure 1.** The structure of the dicationic  $[\text{Au}_{20}(\text{PPhpy}_2)_{10}\text{Cl}_4]^{2+}$  cluster in **1**.

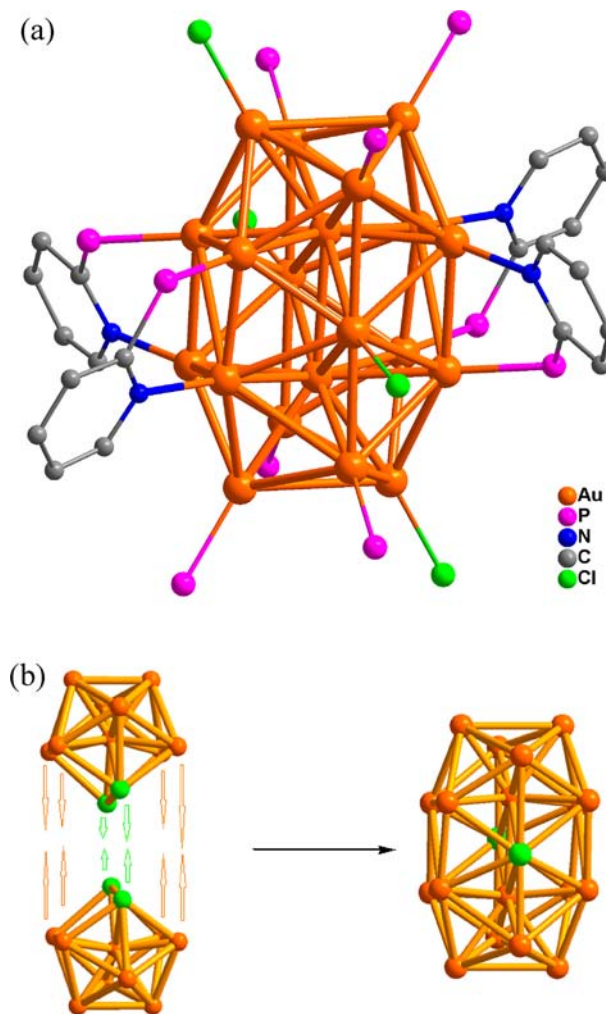


**Figure 2.** (a) The bridging mode of  $\text{PPhpy}_2$  in **1**; phenyl and pyridyl groups not linked to Au atoms have been omitted for clarity. (b) Anatomy of the  $\text{Au}_{20}$  core structure in **1**, two green atoms denote the shared vertices.

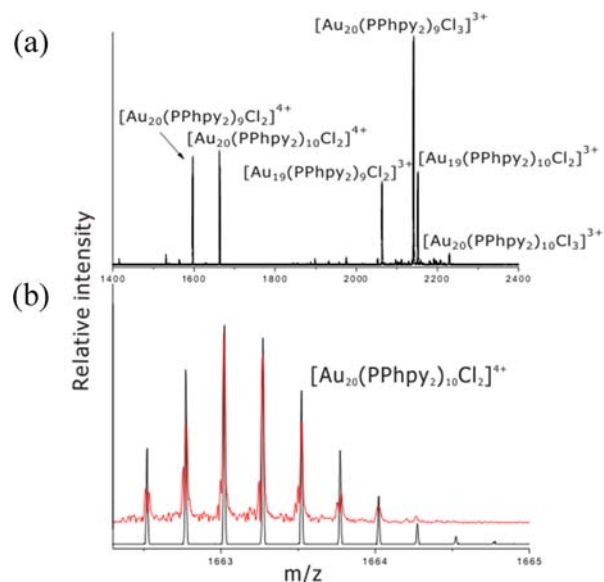


**Figure 3.** (a) Mass spectrum of the  $\text{Au}_{20}$  cluster. (b) The measured (red trace) and simulated (black trace) isotopic patterns of  $[\text{Au}_{20}(\text{PPhpy}_2)_{10}\text{Cl}_2]^{4+}$ .

1662.985 was observed, which corresponds to  $[\text{Au}_{20}(\text{PPhpy}_2)_{10}\text{Cl}_2]^{4+}$  derived from the removal of two chlorides from  $[\text{Au}_{20}(\text{PPhpy}_2)_{10}\text{Cl}_4]^{2+}$ . The observed isotopic pattern of  $[\text{Au}_{20}(\text{PPhpy}_2)_{10}\text{Cl}_2]^{4+}$  is perfectly in agreement with the simulated one (Figure 3b). Another prominent species observed at  $m/z = 2141.248$  corresponds to  $[\text{Au}_{20}(\text{PPhpy}_2)_9\text{Cl}_3]^{3+}$ . This observation indicates that chloride and phosphine ligands can be readily dissociated from **1**.

This  $\text{Au}_{20}$  cluster is quite stable. It is confirmed by UV–vis spectra that no decomposition was observed after its solution had been stored under ambient conditions for a week. The fragmentation pattern in Figure 3 also shows that the  $\text{Au}_{20}$  skeleton can be retained under the ionization conditions with the leave of chloride or phosphine ligands.

The total number of valence electrons of  $[\text{Au}_{20}(\text{PPhpy}_2)_{10}\text{Cl}_4]^{2+}$  is calculated to be 14 ( $n = 20 - 4 - 2$ ). It does not match a case of shell closure, which suggests that  $\text{Au}_{20}$  is stabilized by geometrical factors. The bridging of PN donors of hemilabile phosphines makes large contribution to the stabilization of the nanocluster.

It was reported that bare  $\text{Au}_{20}$  has a tetrahedral ( $T_d$ ) structure with a HOMO–LUMO energy gap of 1.77 eV.<sup>14</sup> Wang et al. identified the composition of a phosphine-protected  $\text{Au}_{20}$  to be  $\text{Au}_{20}(\text{PPh}_3)_8^{2+}$  by mass spectrometry, which was computed to have tetrahedral structure.<sup>15</sup> Jin et al. reported a thiolate-protected  $\text{Au}_{20}$  cluster with a composition of  $\text{Au}_{20}(\text{SCH}_2\text{CH}_2\text{Ph})_{16}$ , which was also determined by mass spectrometry, and the structure has not been determined.<sup>16</sup> Zen et al. performed a calculation on this  $\text{Au}_{20}$  cluster, and predicted that it has a prolate  $\text{Au}_8$  core and four  $-\text{RS}-\text{Au}-\text{RS}-\text{Au}-\text{RS}-\text{Au}-\text{RS}-$  extended staple motifs.<sup>17</sup> The present work represents the first structural determination of a  $\text{Au}_{20}$  cluster.

The UV–vis absorption spectrum of **1** in  $\text{CH}_2\text{Cl}_2$  shows three prominent absorption bands at 493, 344 (shoulder), and 260 nm. The 260 nm band comes from the intraligand transition of the  $\text{PPhpy}_2$  ligand, as a similar band is found in a  $\text{CH}_2\text{Cl}_2$  solution of pure  $\text{PPhpy}_2$ . The optical energy gap was determined to be 2.24 eV (Figure 4 inset), which is much higher than 1.77 eV found in bare  $\text{Au}_{20}$ . It is noteworthy that

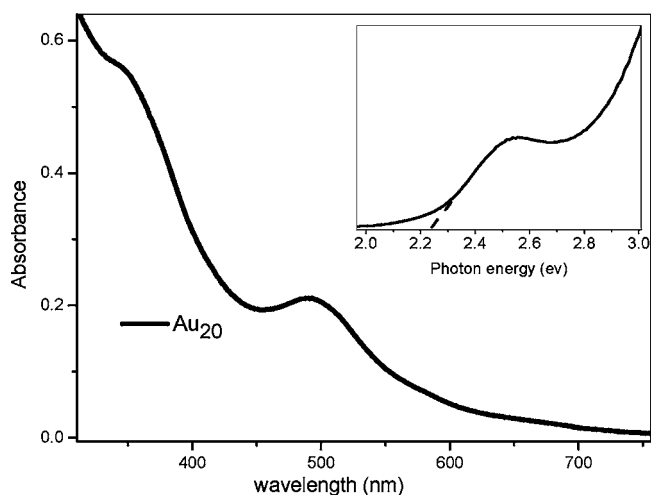


**Figure 4.** The optical absorption spectrum of **1** in methylene dichloride. (Inset) The spectrum on the energy scale (eV); the HOMO–LUMO gap is 2.24 eV.

the absorption profile of **1** is quite similar to that of  $\text{Au}_{20}(\text{SCH}_2\text{CH}_2\text{Ph})_{16}$ , and the HOMO–LUMO gap of **1** is just a little higher than that in  $\text{Au}_{20}(\text{SCH}_2\text{CH}_2\text{Ph})_{16}$  (2.15 eV).

This work demonstrates that a new cluster core  $\text{Au}_{20}$  has been obtained with the use of hemilabile phosphines. The bridging ability of hemilabile phosphines enhances the stability of the  $\text{Au}_{20}$ . The arrangement of the  $\text{Au}_{20}$  core structure suggests that the incomplete icosahedral motifs may be taken into consideration in making prediction of the structures of gold clusters.

## ■ ASSOCIATED CONTENT

### 📄 Supporting Information

Synthesis and characterization details. This material is available free of charge via the Internet at <http://pubs.acs.org>.

## ■ AUTHOR INFORMATION

### Corresponding Author

qmwang@xmu.edu.cn

### Notes

The authors declare no competing financial interest.

## ■ ACKNOWLEDGMENTS

This work was supported by the Natural Science Foundation of China (21125102, 20973135, 90922011 and 21021061).

## ■ REFERENCES

- (1) (a) Häkkinen. *Nat. Chem.* **2012**, *4*, 443. (b) Jin, R. C.; Zhu, Y.; Qian, H. F. *Chem.—Eur. J.* **2011**, *17*, 6584. (c) Parker, J. F.; Fields-Zinna, C. A.; Murry, R. W. *Acc. Chem. Res.* **2010**, *43*, 1289. (d) Schmid, G. *Chem. Soc. Rev.* **2008**, *37*, 1909. (e) Wilcoxon, J. P.; Abrams, B. L. *Chem. Soc. Rev.* **2006**, *35*, 1162. (f) Daniel, M.-C.; Astruc, D. *Chem. Rev.* **2004**, *104*, 293.
- (2) For example: (a) Qian, H. F.; Zhu, Y.; Jin, R. C. *Proc. Natl. Acad. Sci. U.S.A.* **2012**, *109*, 696. (b) Negishi, Y.; Takasugi, Y.; Sato, S.; Yao, H.; Kimura, K.; Tsukuda, T. *J. Am. Chem. Soc.* **2004**, *126*, 6518. (c) Nimmala, P. R.; Dass, A. *J. Am. Chem. Soc.* **2011**, *133*, 9175.
- (3) Jadzinsky, P. D.; Calero, G.; Ackerson, C. J.; Bushnell, D. A.; Kornberg, R. D. *Science* **2007**, *19*, 430.
- (4) (a) Heaven, M. W.; Dass, A.; White, P. S.; Holt, K. M.; Murray, R. W. *J. Am. Chem. Soc.* **2008**, *130*, 3754. (b) Zhu, M.; Aikens, C. M.; Hollander, F. J.; Schatz, G. C.; Jin, R. *J. Am. Chem. Soc.* **2008**, *130*, 5883.

(5) Qian, H.; Eckenhoff, W. T.; Zhu, Y.; Pintauer, T.; Jin, R. *J. Am. Chem. Soc.* **2010**, *132*, 8280.

(6) (a) Hall, K. P.; Mingos, M. P. *Prog. Inorg. Chem.* **1984**, *32*, 237. (b) Laguna, A.; Laguna, M.; Gimeno, M. C.; Jones, P. G. *Organometallics* **1992**, *11*, 2759. (c) McPartlin, M.; Mason, R.; Malatesta, L. *J. Chem. Soc. D* **1969**, 334. (d) Van der Velden, J. W. A.; Vollenbroek, F. A.; Bour, J. J.; Beuskens, P. I.; Smits, J. M. M.; Bosman, W. P. *Recl.: J. R. Neth. Chem. Soc.* **1981**, *100*, 148. (e) Shichibu, Y.; Konishi, K. *Small* **2010**, *6*, 1216.

(7) Guidez, E. B.; Hadley, A.; Aikens, C. M. *J. Phys. Chem. C* **2011**, *115*, 6305.

(8) Pettibone, J. M.; Hudgens, J. W. *ACS Nano* **2011**, *5*, 2989.

(9) Teo, B. K.; Shi, X.; Zhang, H. *J. Am. Chem. Soc.* **1992**, *114*, 2743.

(10) Akola, J.; Walter, M.; Whetten, R. L.; Häkkinen, H.; Grönbeck, J. *J. Am. Chem. Soc.* **2008**, *130*, 3756.

(11) Shichibu, Y.; Negishi, Y.; Watanabe, T.; Chaki, N. K.; Kawaguchi, H.; Tsukuda, T. *J. Phys. Chem. C* **2007**, *111*, 7845.

(12) (a) Teo, B. K.; Hong, M.; Zhang, H.; Huang, D.; Shi, X. *J. Chem. Soc., Chem. Commun.* **1988**, 204. (b) Nunokawa, K.; Ito, M.; Sunahara, T.; Onaka, S.; Ozeki, T.; Chiba, H.; Funahashi, Y.; Masuda, H.; Yonezawa, T.; Nishihara, H.; Nakamoto, M.; Yamamoto, M. *Dalton Trans.* **2005**, 2726.

(13) Crystal data for  $\text{1} \cdot 2\text{CH}_2\text{Cl}_2 \cdot 4\text{MeOH} \cdot 4\text{H}_2\text{O}$ ,  $\text{C}_{160}\text{H}_{130}\text{Cl}_6\text{N}_{20}\text{P}_{10}\text{Au}_{20} \cdot 2\text{CH}_2\text{Cl}_2 \cdot 4\text{MeOH} \cdot 4\text{H}_2\text{O}$ ,  $a = 17.5796(5)$ ,  $b = 18.0261(5)$ ,  $c = 18.1007(6)$  Å,  $\alpha = 118.070(3)$ ,  $\beta = 94.307(2)$ ,  $\gamma = 110.248(3)^\circ$ ,  $V = 4548.1(2)$  Å<sup>3</sup>, space group  $\text{P}\bar{1}$ ,  $Z = 1$ ,  $T = 173$  K, 50 356 reflections measured, 21 489 unique ( $R_{\text{int}} = 0.0985$ ), final  $R1 = 0.0719$ ,  $wR2 = 0.1308$  for 12748 observed reflections [ $I > 2\sigma(I)$ ].

(14) Li, J.; Li, X.; Zhai, H.-J.; Wang, L.-S. *Science* **2003**, *299*, 864.

(15) Bertino, M. F.; Sun, Z.-M.; Zhang, R.; Wang, L.-S. *J. Phys. Chem. B* **2006**, *110*, 21416.

(16) Pei, Y.; Gao, Y.; Shao, N.; Zeng, X. C. *J. Am. Chem. Soc.* **2009**, *131*, 13619.

(17) Zhu, M.; Qian, H.; Jin, R. *J. Am. Chem. Soc.* **2009**, *131*, 7220.